Spectral efficiency of distributed antenna system with random antenna layout

Hairuo Zhuang, Lin Dai, Liang Xiao and Yan Yao

The downlink capacity potential of a distributed antenna system (DAS) with random antenna layout is investigated. A low complexity sub-optimal power allocation scheme among transmit antennas is proposed. Simulation results show that with the same antenna density DAS outperforms a co-located antenna system (CAS) in terms of average and outage spectral efficiency.

Introduction: Many previous studies of distributed antenna systems (DAS) have focused on the macroscopic diversity advantage to combat large-scale fading and improve coverage and link quality [1]. In this Letter, we are motivated to investigate the downlink capacity potential of DAS as a multiple-input multiple-output (MIMO) system. In the downlink of DAS, the transmit antennas are spatially distributed around the subscriber equipped with M co-located receive antennas. There is no specific signal processing at the distributed antennas except for RF amplification, frequency translation and possibly optic-electric conversion. Through optical fibres or coaxial cables these antennas are connected to a central processor where all complex signal processing is performed. By measuring the local mean receive power of each distributed antenna in the uplink, the central processor selects the strongest N distributed antennas for downlink transmission simultaneously and on the same frequency. We use the following flat-fading quasi-static model for analysis

$$\mathbf{y} = \mathbf{H}_w\mathbf{F}\mathbf{x} + \mathbf{n} \tag{1}$$

where $\mathbf{x}$ and $\mathbf{y}$ are the transmit and receive vectors, respectively, and $\mathbf{n}$ is the noise vector with i.i.d. $\tilde{N}(0, \sigma^2)$ entries. The small-scale fast fading is denoted by an $M \times N$ matrix $\mathbf{H}_w$ with i.i.d. $\tilde{N}(0, 1)$ entries. Unlike the conventional co-located antenna system (CAS), in DAS, the transmit antennas suffer from different degrees of large-scale fading, denoted by a local stationary $N \times N$ diagonal matrix $\mathbf{F}$. In the following, we assume that large-scale fading is only determined by the path loss, i.e. $\mathbf{F} = \text{diag}\,(d_1^{-\gamma/2}, d_2^{-\gamma/2}, \ldots, d_N^{-\gamma/2})$, where d_i is the access distance between the subscriber and the ith nearest distributed antenna and γ is the path loss exponent. We assume that $\mathbf{F}$ is available at the transmitter, which is reasonable due to the mechanism of antenna selection in DAS.

Random antenna layout: Since the path losses to different transmit antennas may change as the subscriber moves to different locations, a key problem is to investigate the characteristics of the access distances. Unfortunately, the access distances of DAS are related to the antenna layout, which may vary with system configurations and specific environments [1]. To provide a more general model, here we treat this problem using a random antenna layout. We believe that, with no intention to optimise the antenna layout, the performance of a random antenna layout roughly represents a lower bound. Moreover, owing to the complex landform of real environments, regular antenna layout is difficult to realise in practice and some sort of randomness is exhibited.

Consider a circular area with radius r, where there are a total of n antennas, each of which is randomly located in this area with uniform probability independent of other antennas. We assume without loss of generality that the subscriber is located at the centre of the circular area. It is straightforward to write the cumulative distribution function of the shortest access distance d_1

$$F_{d_1}(x) = \Pr(d_1 < x) = 1 - \left(1 - \frac{x^2}{r^2}\right)^n, \quad 0 < x \le r \tag{2}$$

We are most interested in the asymptotic behaviour of d_1 as r and n go to infinity while keeping the antenna density $\lambda \triangleq n/\pi r^2$ as a finite constant. Upon taking limits and the differential in (2) we derive the asymptotic probability density function (PDF) of d_1

$$f_{d_1}(x) = 2\pi\lambda x \cdot e^{-\pi\lambda x^2} \tag{3}$$

Similarly, we have the conditional PDF of d_i $(i \ge 2)$

$$f_{d_i}(x|d_{i-1}) = 2\pi\lambda x \cdot e^{-\pi\lambda(x^2 - d_{i-1}^2)}, \quad i \ge 2 \tag{4}$$

Interestingly, if we let $d_0 = 0$, we note the following simple relation of these variables

$$d_i = \sqrt{d_{i-1}^2 + \eta_i}, \quad i = 1, 2, 3, \ldots \tag{5}$$

where η_i are independent random variables with negative exponential distributions

$$f_{\eta_i}(x) = \pi\lambda \cdot e^{-\pi\lambda x}, \quad i = 1, 2, 3, \ldots \tag{6}$$

To gauge and compare the access qualities of DAS and CAS, we define the mean square access distance (MSAD) as $\overline{d^2} \triangleq (1/N)\sum_{i=1}^{N} d_i^2$. It is a random variable that roughly reflects the overall degree of path loss. We are interested in the first-order and second-order statistics of MSAD. After some algebra, we have $E(\overline{d_{DAS}^2}) = (N+1)/2\pi\lambda$. and Var $(\overline{d_{DAS}^2}) = (N+1)(2N+1)/6N\pi^2\lambda^2$. In CAS, the subscriber always communicates with the nearest base station in which N antennas are co-located. Thus the access distance distribution of random base station layout with the same antenna density as DAS follows from (3) by replacing λ with λ/N. Thus $E(\overline{d_{CAS}^2}) = N/\pi\lambda$ and Var $(\overline{d_{CAS}^2}) = N^2/\pi^2\lambda^2$. Obviously the expectation and variance of MSAD in DAS are smaller than those in CAS as $N \ge 2$. This implies that DAS would achieve higher mean spectral efficiency and would be less sensitive to the location of the subscriber than CAS with the same antenna density.

Power allocation among antennas: It is well known that for CAS, uniform power allocation is optimal when the channel state information is not available at the transmitter. However, in DAS, with $\mathbf{F}$ known at the transmitter, uniform power allocation is not optimal due to the different path loss of each distributed antenna. From [3], the mutual information is given by

$$I(\mathbf{Q}) = \log_2\det\left(\mathbf{I} + \frac{1}{\sigma^2}\mathbf{H}_w\mathbf{F}\mathbf{Q}\mathbf{F}^H\mathbf{H}_w^H\right) \tag{7}$$

where $\mathbf{Q} = E(\mathbf{x}\mathbf{x}^H)$ is the transmit covariance matrix. With $\mathbf{F}$ available at the transmitter, it has been proved in [2] that the optimal $\mathbf{Q}$ obtaining the capacity $C(P) = \max_{\mathbf{Q}:tr(\mathbf{Q})=P} E[I(\mathbf{Q})]$ must be a diagonal matrix, i.e. $\mathbf{Q} = \text{diag}(P_1, P_2, \ldots, P_N)$ with power constraint $\sum_{i=1}^{N} P_i = P$. However, the optimal allocation of P needs numerical optimisation that is of high complexity. Thus we derive a low complexity allocation scheme that maximises the upper bound of $E[I(\mathbf{Q})]$. For conciseness, let $\mathbf{T} = (1/\sigma^2)\mathbf{H}_w\mathbf{F}\mathbf{Q}\mathbf{F}^H\mathbf{H}_w^H$. The following upper bound can be derived

$$\begin{aligned} E[I(\mathbf{Q})] &= E[\log_2\det(\mathbf{I} + \mathbf{T})] \le E\left[\log_2\textstyle\prod_{i=1}^{N}(1 + [\mathbf{T}]_{ii})\right] \\ &= \sum_{i=1}^{N} E[\log_2(1 + [\mathbf{T}]_{ii})] \le \sum_{i=1}^{N}\log_2 E(1 + [\mathbf{T}]_{ii}) \\ &= \sum_{i=1}^{N}\log_2\left(1 + \frac{P_i N}{\sigma^2 d_i^2}\right) \end{aligned} \tag{8}$$

where the first inequality draws from the fact that for any positive definite matrix $\mathbf{A}$, $\det(\mathbf{A}) \le \prod_i [\mathbf{A}]_{ii}$ and the second one follows from $E(\log X) \le \log(E(X))$ since $\log X$ is a concave function. The power allocation scheme that maximises the upper bound in (8) is then solved using a water-filling principle [3], that is

$$P_i = \left(\mu - \frac{\sigma^2 d_i^2}{N}\right)^+ \quad i = 1, 2, \ldots, N \tag{9}$$

where μ is chosen to satisfy $\sum_{i=1}^{N} P_i = P$. Detailed simulations show that the performance of this low complexity allocation scheme is quite close to the optimal one obtained by numerical optimisation. Thus we refer to this scheme as a sub-optimal one.

Simulation results and conclusions: We plot the average spectral efficiency C_{mean} and 10% outage spectral efficiency $C_{0.1}$ of DAS by Monte Carlo simulations. The signal-to-noise ratio (SNR) is given by P/σ^2. We adopt the distribution of d_i in (3)–(6). Both uniform power allocation and the sub-optimal power allocation scheme are simulated. For comparison, the results of CAS with the same antenna density and random base station distribution are also presented, where we assume there is no correlation between transmit antennas. In practice, correlation between transmit antennas will result in capacity degradations in CAS [2].

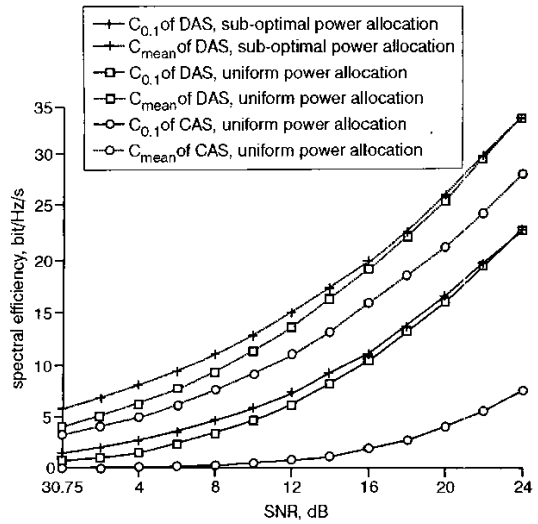

Fig. 1 *Spectral efficiency comparison of DAS and CAS, $M=8$, $N=8$*

Fig. 1 shows the results for $M=8$, $N=8$, $\gamma=3.7$ and $\lambda=1/\pi$. Note that the choice of λ is trivial since it only results in the shift of all curves along SNR axis. The following observations can be concluded: (i) DAS obtains higher mean spectral and outage spectral efficiency than CAS. This partially attributes to the smaller expectation of MSAD in DAS. (ii) The gap between the C_{mean} and $C_{0.1}$ in DAS is smaller than that in CAS, demonstrating that the spectral efficiency of DAS is less sensitive to the location of the subscriber. This coincides with our analysis of the variance of MSAD. (iii) Using our proposed power allocation scheme, the spectral efficiency is further increased compared with uniform power allocation. The improvement is more evident at low SNRs than at high SNRs where water-filling is almost reduced to uniform power allocation.

Acknowledgment: This work is supported by China Nature Science Foundation (90204001) and ETRI of Korea.

12 February 2003
Electronics Letters Online No: 20030327
DOI: 10.1049/el:20030327

Hairuo Zhuang, Lin Dai, Liang Xiao and Yan Yao (*State Key Lab on Microwave and Digital Communications, Department of Electronics Engineering, Tsinghua Univ., Beijing 100084, P.R. China*)

E-mail: zhr@wireless.mdc.tsinghua.edu.cn

References

1 WEISS, U.: 'Designing macroscopic diversity cellular systems'. Vehicular Technology Conference, 1999 IEEE 49th, July 1999, Vol. 3, pp. 2054–2058
2 JAFAR, S., and GOLDSMITH, S.: 'Transmitter optimization and optimality of beamforming for multiple antenna system with imperfect feedback', *IEEE Trans. Wireless Commun.* (to be published)
3 TELATAR, E.: 'Capacity of multi-antenna Gaussian channels'. AT&T Bell Labs Internal Tech. Memo., June 1995

Switched-capacitor realisation of Lorenz-type chaotic systems

S. Özoğuz

It is shown that a recently reported Lorenz-type chaotic system with switching-type nonlinearities can be effectively realised using the switched-capacitor circuit design technique in a simple and straightforward manner. Experimental results from a constructed circuit capable of generating the complex (four-wing) butterfly attractor are shown.

Introduction: A novel Lorenz-type system capable of generating a complex (four-wing) butterfly attractor was recently reported [1]. This system is multiplier-free and employs only binary switching-type nonlinearities. The realisation given in [1] of this system employs six opamps and two comparators. Considering that a third-order system is typically realised using three opamps, it follows that the technique used in [1] is not optimal.

In this Letter, we give an effective realisation of the system using the switched-capacitor (sC) design technique [2], which is also suitable for monolithic implementation. It turns out that the two nonlinearities of the system can be realised simply by exchanging the clock signals of some switch pairs with no need for extra opamps. Furthermore, if it is only required to realise the modified Lorenz system reported in [3], then two of the clock signals can be spared. It is worth noting that sC circuits have been used to realise chaotic oscillators based on iterated maps [4] and chaotic neurons [5].

Proposed circuit for Lorenz-type system: The Lorenz-type system of [1] is given by:

$$\begin{aligned} \dot{X} &= a(Y-X) \\ \dot{Y} &= -SKZ \\ \dot{Z} &= SKX - S \end{aligned} \tag{1}$$

where $K=\text{sign}(X)$ and $0<a<1$. The system has two complementary modes S_+ and S_- which are selected setting $S=1$ and $S=-1$, respectively. Operating in either S_+ or S_-, the system generates a two-wing butterfly attractor. By forcing the system to switch between these modes, by using an external pulse train with a period $T_P=mT_S$, a complex (four-wing) butterfly attractor is observed. T_S is the normalised time constant of (1) and the typical value of m is 250.

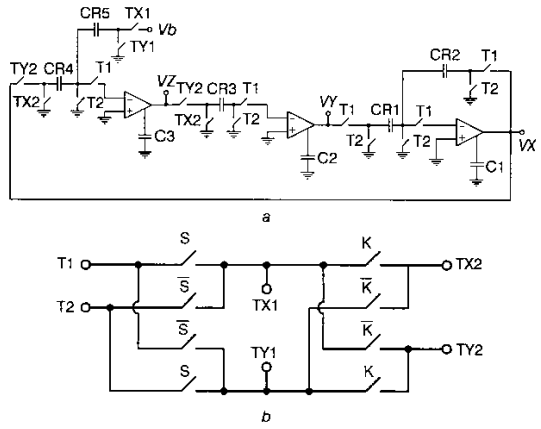

Fig. 1 *Proposed sC realisation of (1), and circuit which generates clock signals*

a Proposed sC realisation of (1)
b Circuit which generates clock signals

Table 1: Truth table for generating clock signals.

S	K	T_{X1}	T_{Y1}	T_{X2}	T_{Y2}
0	0	T_2	T_1	T_1	T_2
0	1	T_2	T_1	T_2	T_1
1	0	T_1	T_2	T_2	T_1
1	1	T_1	T_2	T_1	T_2

The proposed sC circuit realising (1) is shown in Fig. 1*a*; T_1 and T_2 are two non-overlapping clock signals. The nonlinearities required to generate the butterfly attractor simply consist of generating the four clock signals T_{X1}, T_{X2}, T_{Y1} and T_{Y2}, which are determined according to Table 1. This truth table can be realised using the simple switched circuit in Fig. 1*b*. As seen from this Figure, the clock signal pairs $T_{X1}-T_{Y1}$ and $T_{X2}-T_{Y2}$ become either T_1-T_2 or T_2-T_1 according to the values of K and S. So, the required nonlinearities is realised in a very simple manner by exchanging the clock signals of the switch pairs controlled by $T_{X1}-T_{Y1}$ and $T_{X2}-T_{Y2}$.